

Structural Engineering of Metal-organic Framework Derived Tin Sulfides for Advanced Li/Na Storage

*Qiaohuan Cheng, and Xuebin Yu**

Department of Materials Science, Fudan University, Shanghai 200433, P. R. China

*Corresponding Author: E-mail: yuxuebin@fudan.edu.cn (X. B. Yu)

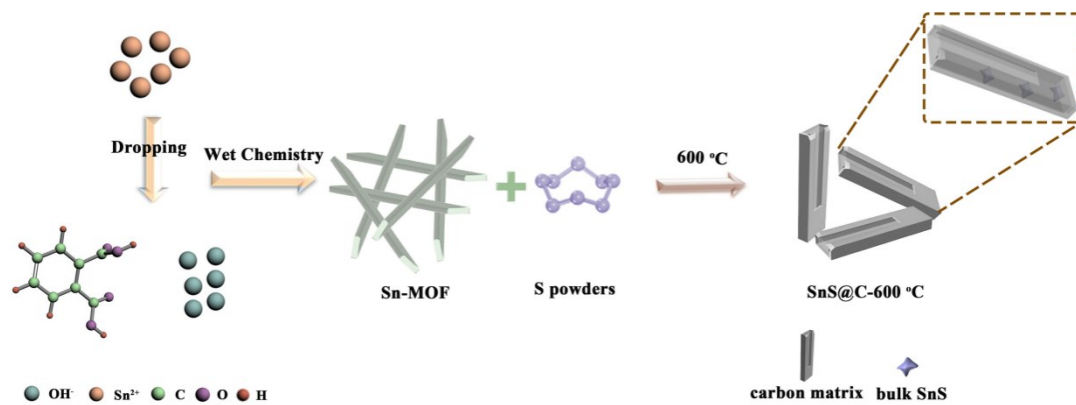


Fig. S1 Schematic illustration of the fabrication process of SnS@C-600 °C.

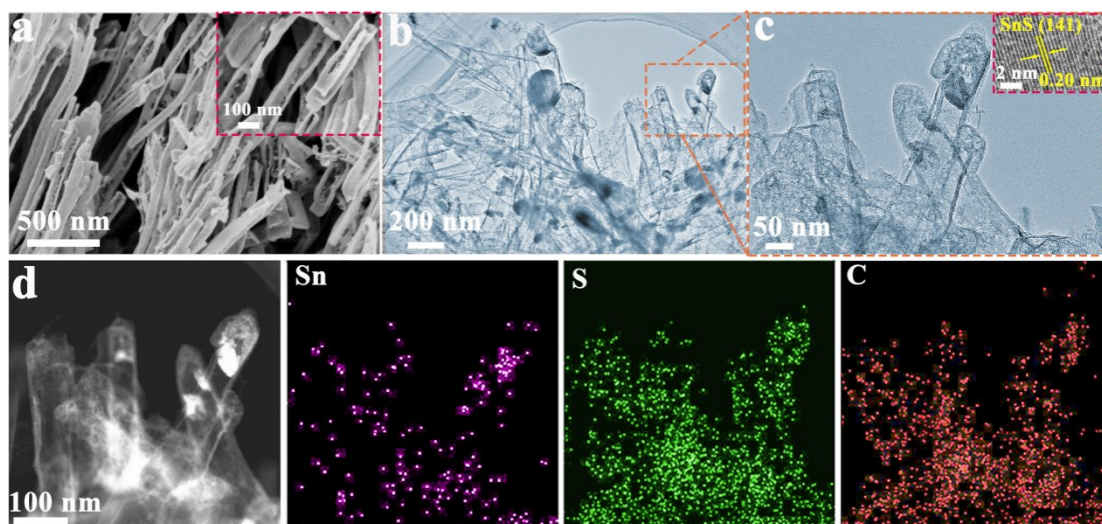


Fig. S2 Morphology characterization of SnS@C-600 °C. (a) SEM image, (b) TEM image, (c) HRTEM image and (d) STEM image and the elemental mappings of SnS@C-600 °C. The inset of (a) and (c) are SEM and HRTEM images of SnS@C-600 °C, respectively.

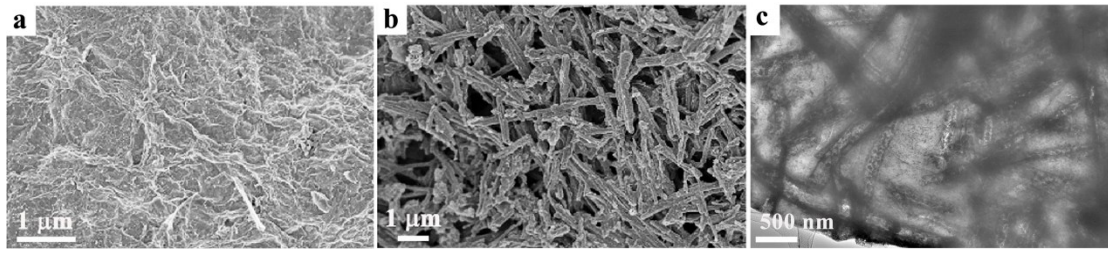


Fig. S3 SEM images of (a) SnS@C/rGO and (b) SnS@NC, (c) TEM image of SnS@NC.

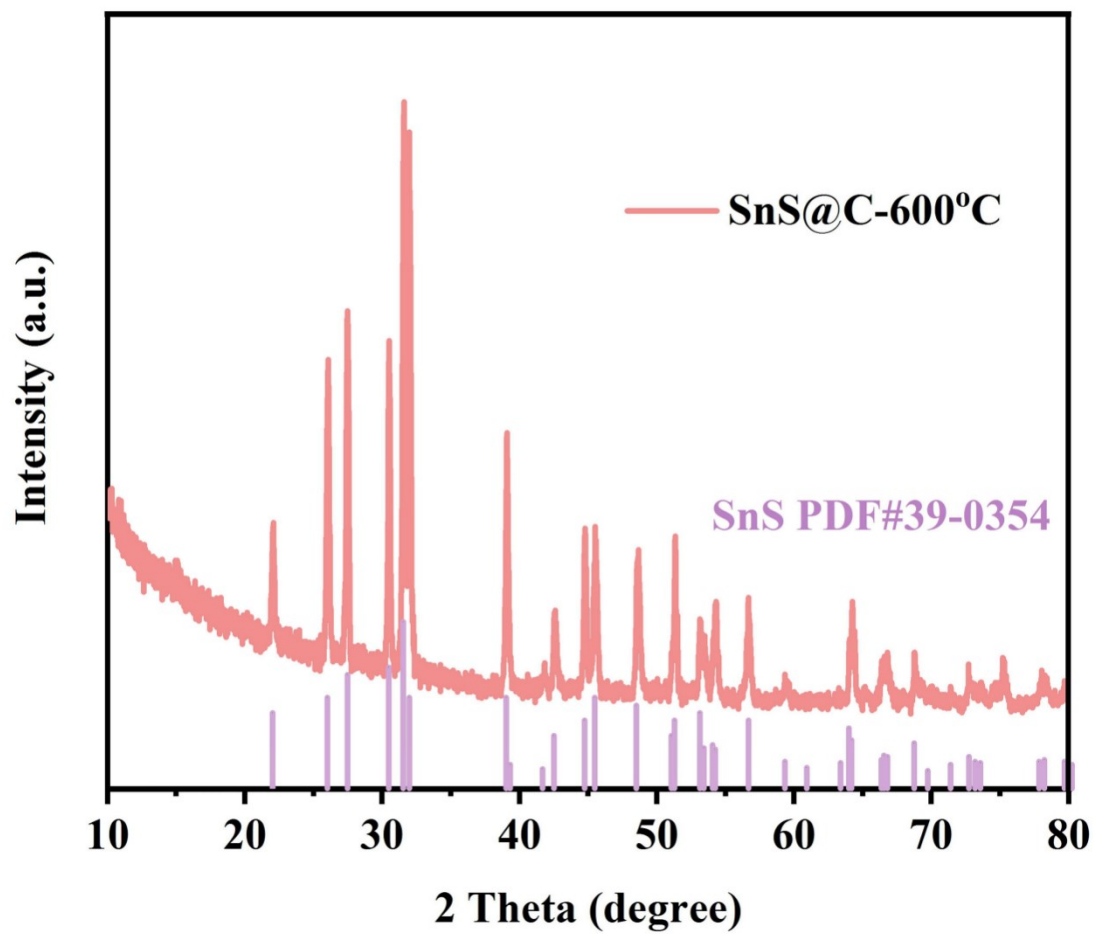


Fig. S4 XRD pattern of SnS@C-600 °C.

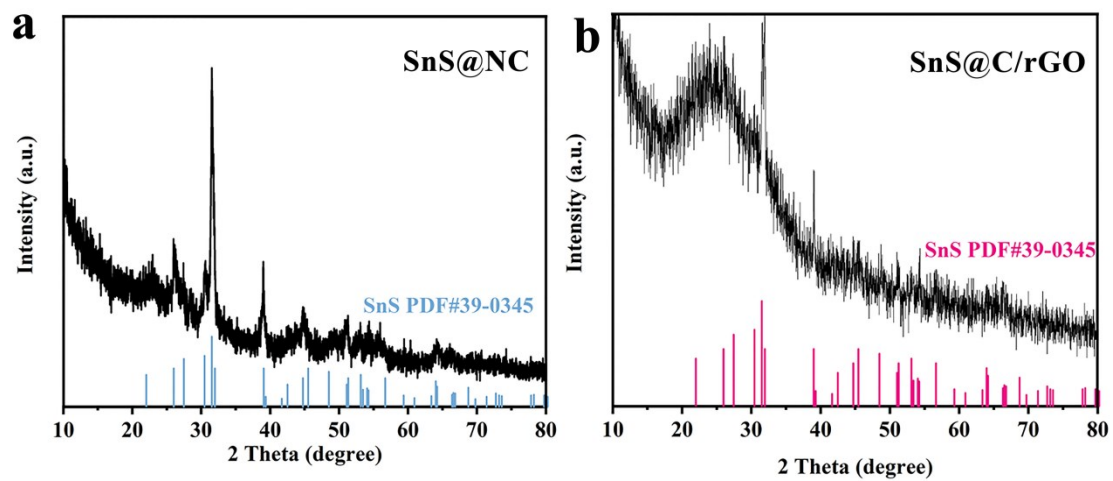


Fig. S5 XRD patterns of (a) SnS@NC and (b) SnS@C/rGO.

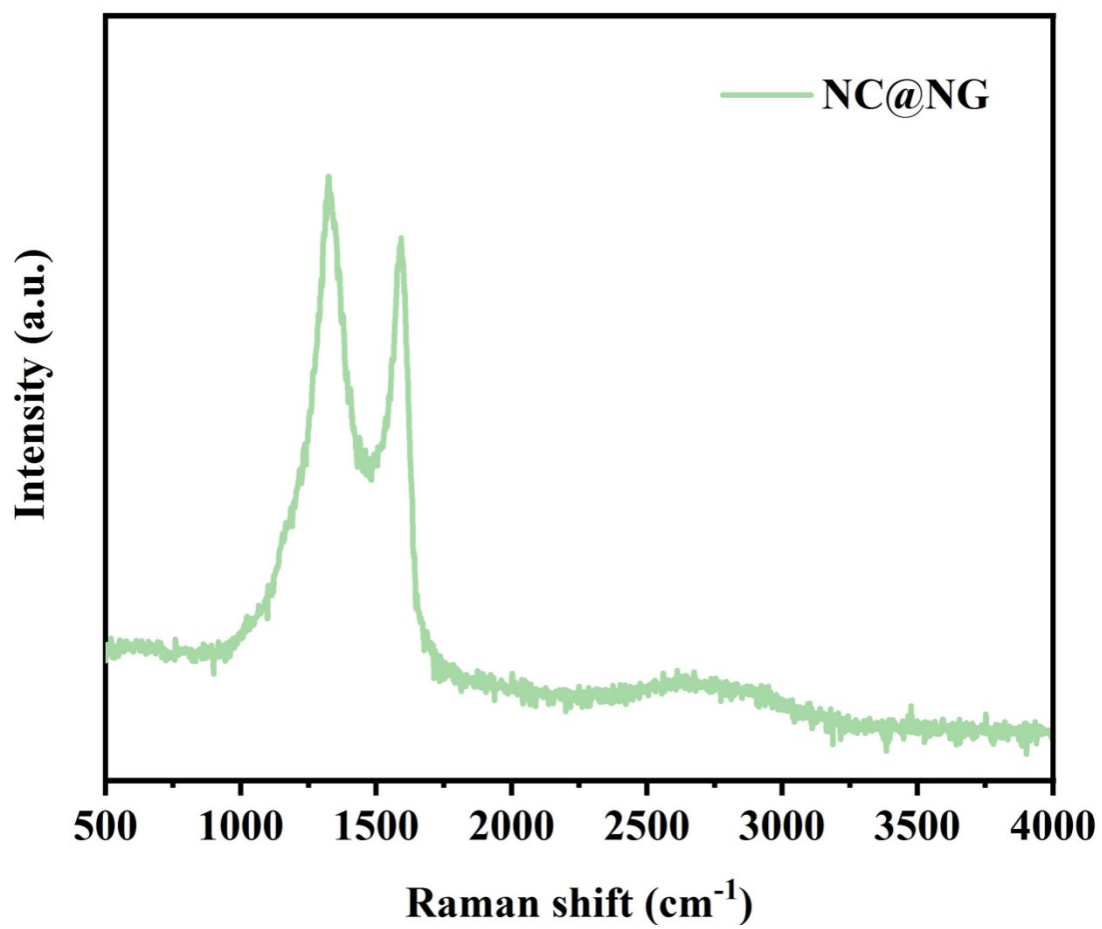


Fig. S6 Raman scattering spectrum of NC@NG.

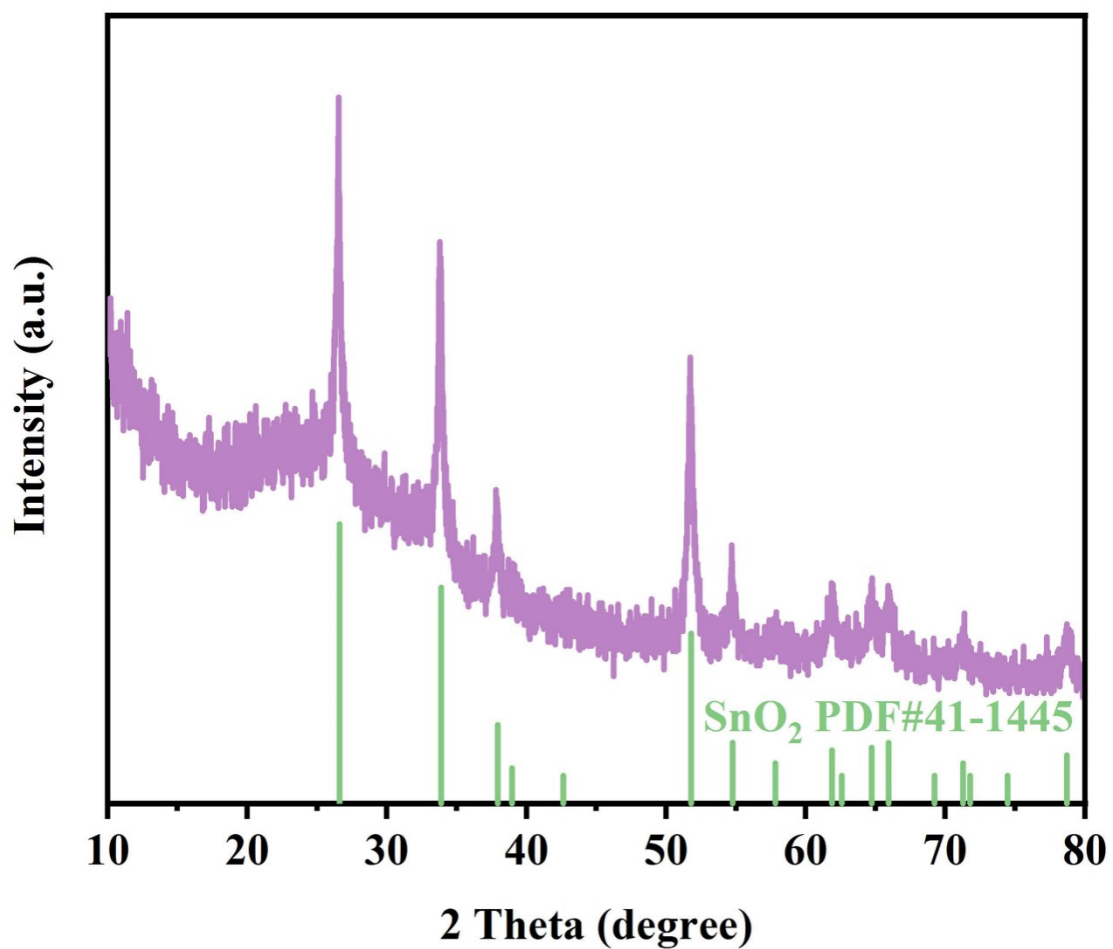


Fig. S7 XRD pattern of powers obtained by calcining SnS@NC@NG in air to 800 °C (the XRD patterns of all samples after being calcined in air to 800 °C are the same with this pattern except for intensity).

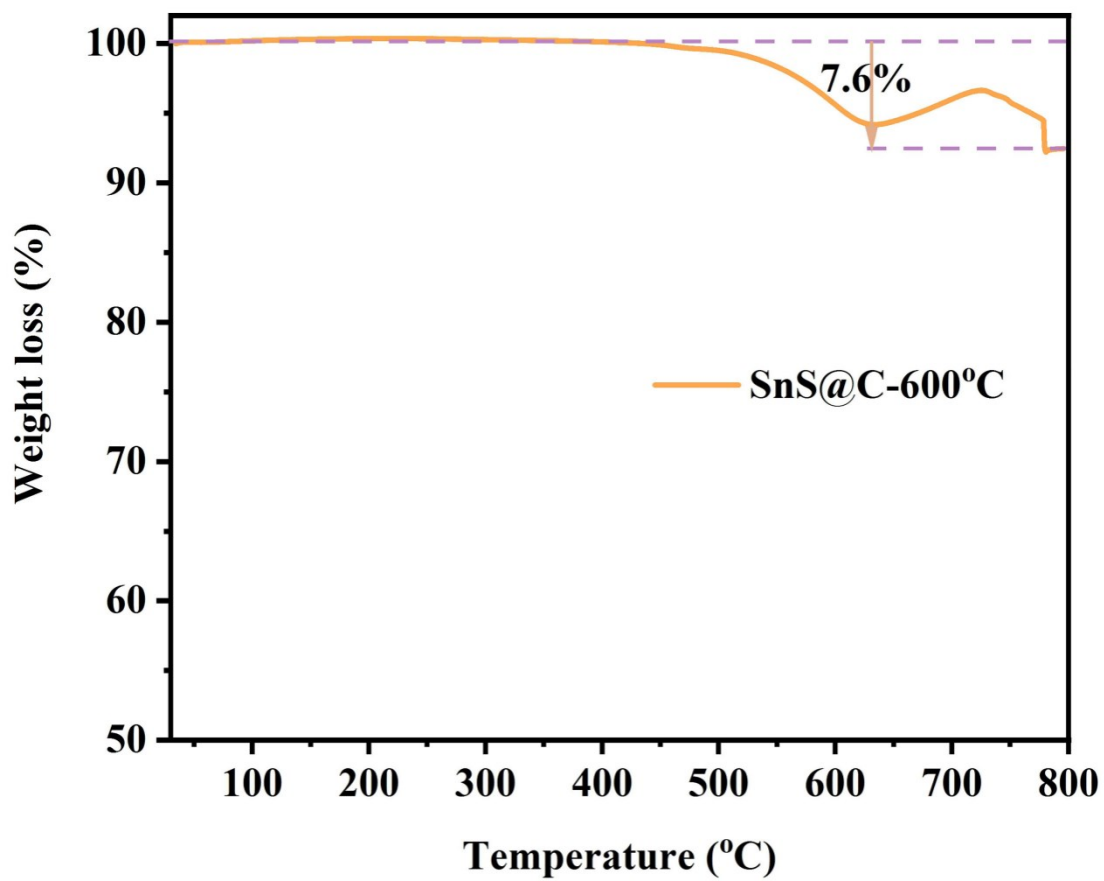


Fig. S8 TGA curve of SnS@C-600 °C.

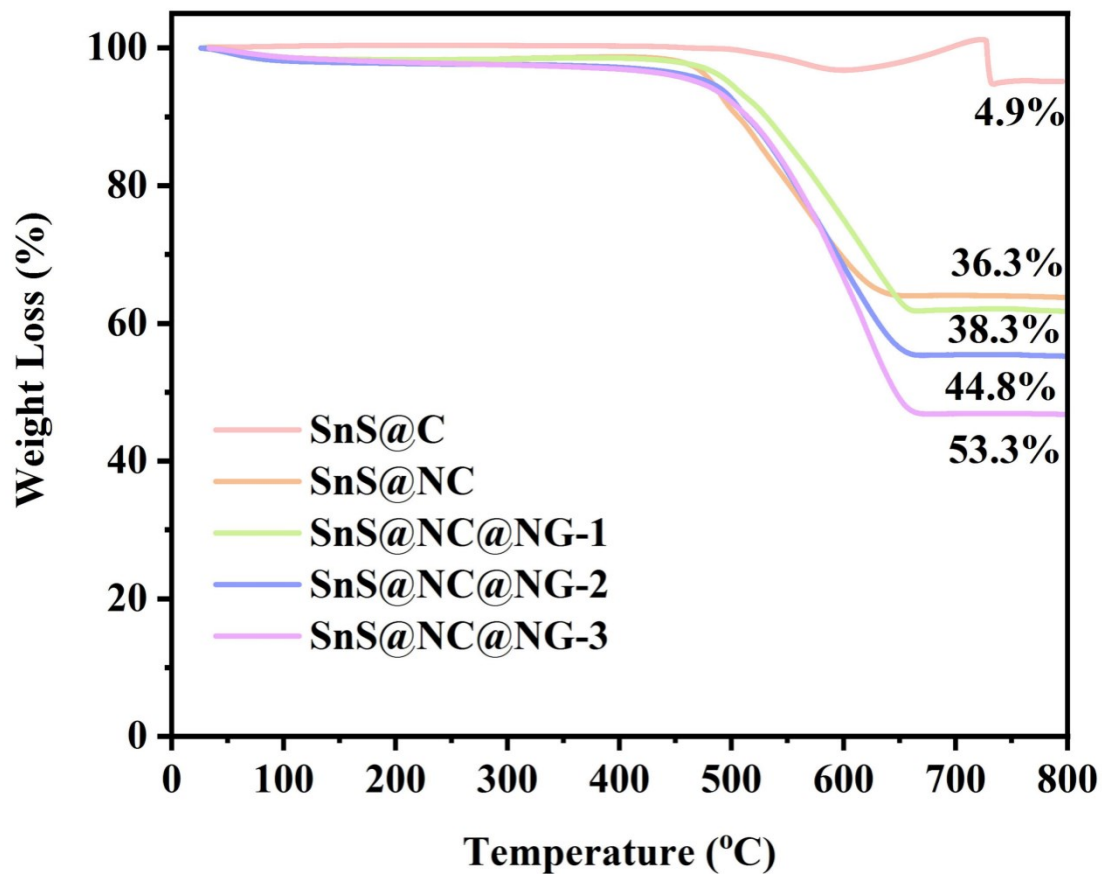


Fig. S9 TGA curves of SnS@C, SnS@NC, SnS@NC@NG-1, SnS@NC@NG-2 and SnS@NC@NG-3, respectively.

The NG content of SnS@NC@NG-1, SnS@NC@NG-2 and SnS@NC@NG-3 is calculated to be 2 wt%, 8.5 wt% and 17 wt%, respectively.

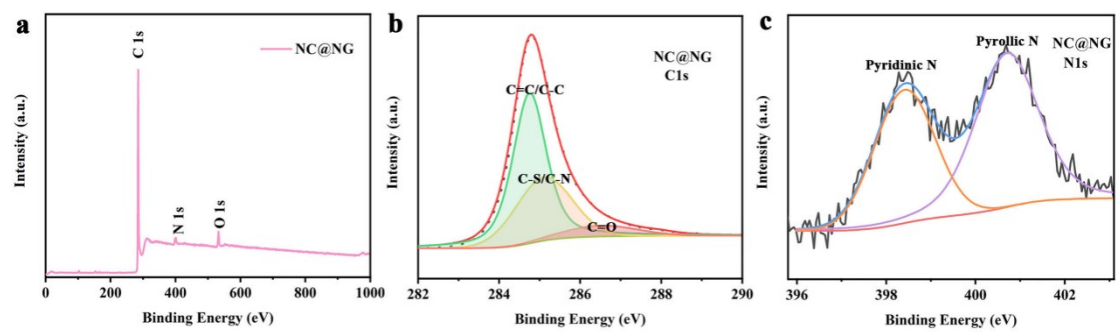


Fig. S10 XPS survey of the NC@NG (a) and its high-resolution spectra: (b) C 1s and (c) N 1s.

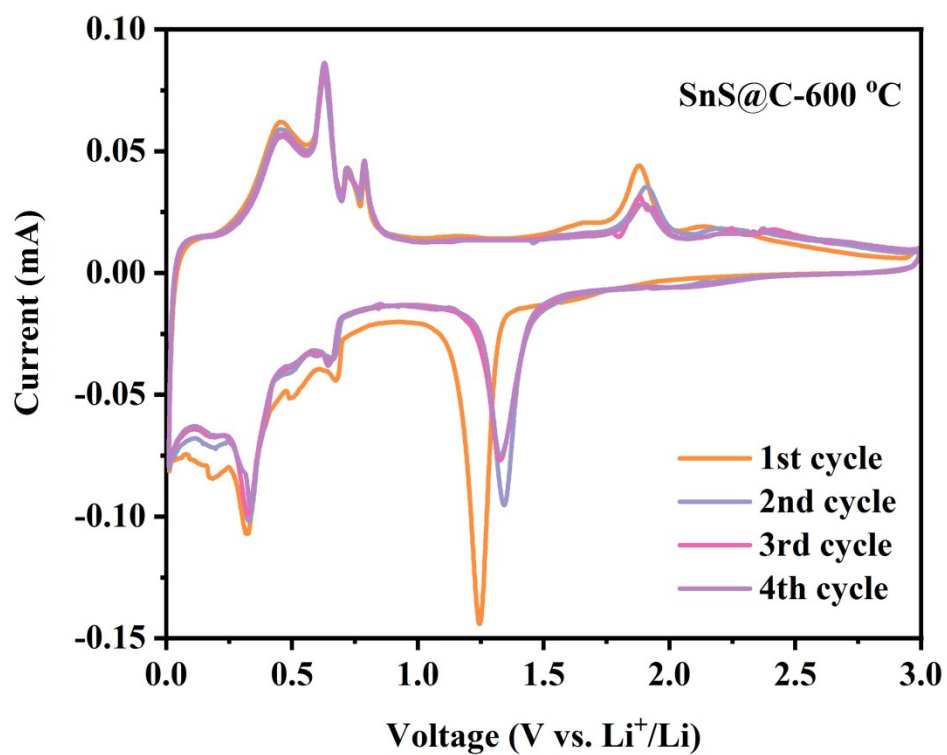


Fig. S11 CV curves of SnS@C-600 °C at 0.1 mV s⁻¹.

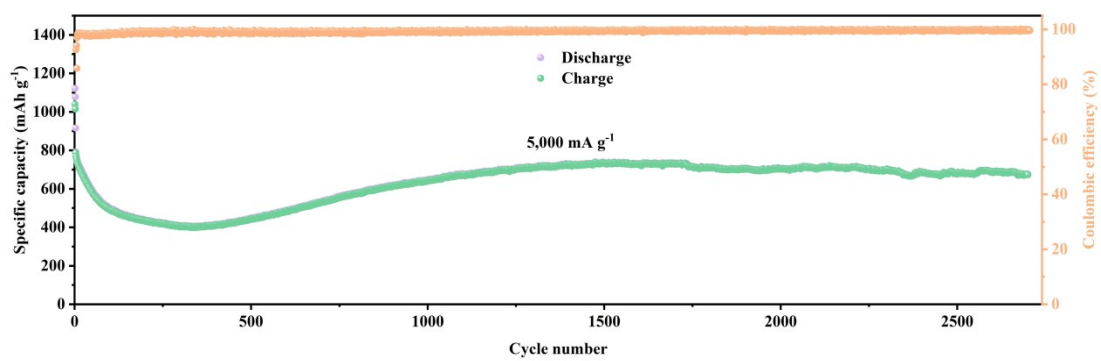


Fig. S12 Cycling performance of SnS@C-600 °C at a current density of 5 A g⁻¹ for LIBs.

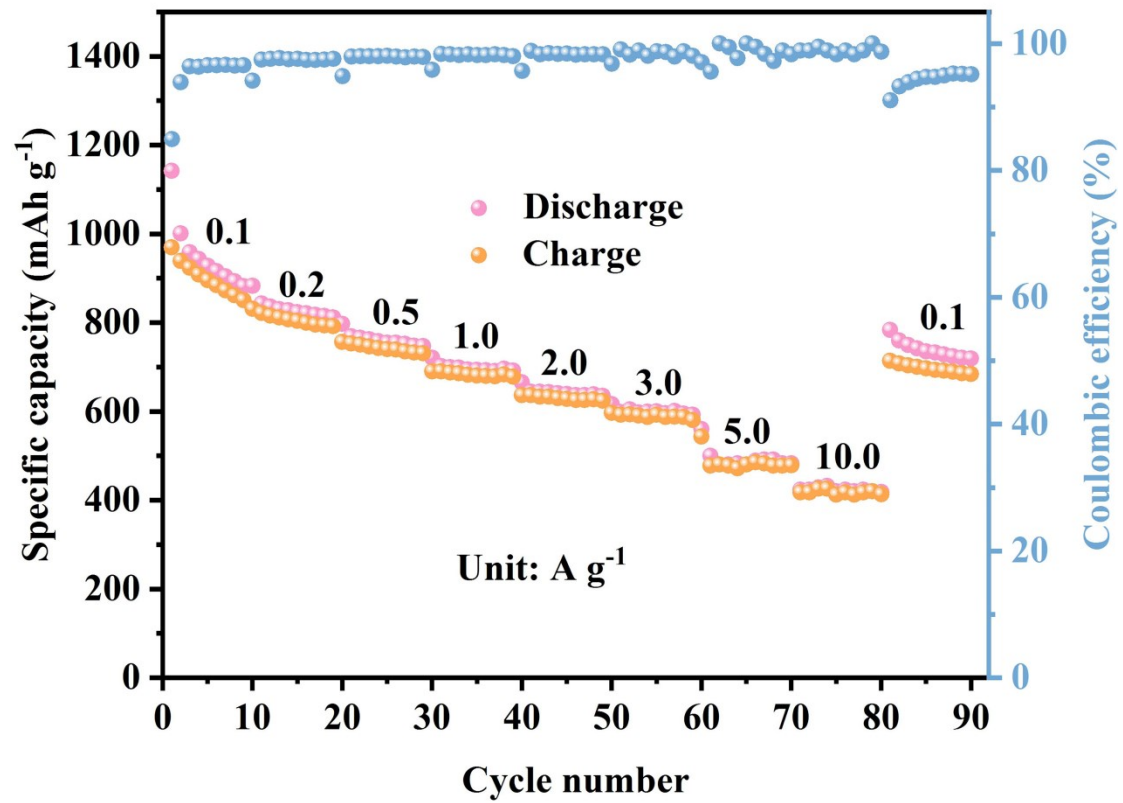


Fig. S13 Rate performance of SnS@C-600 °C at various current density for LIBs.

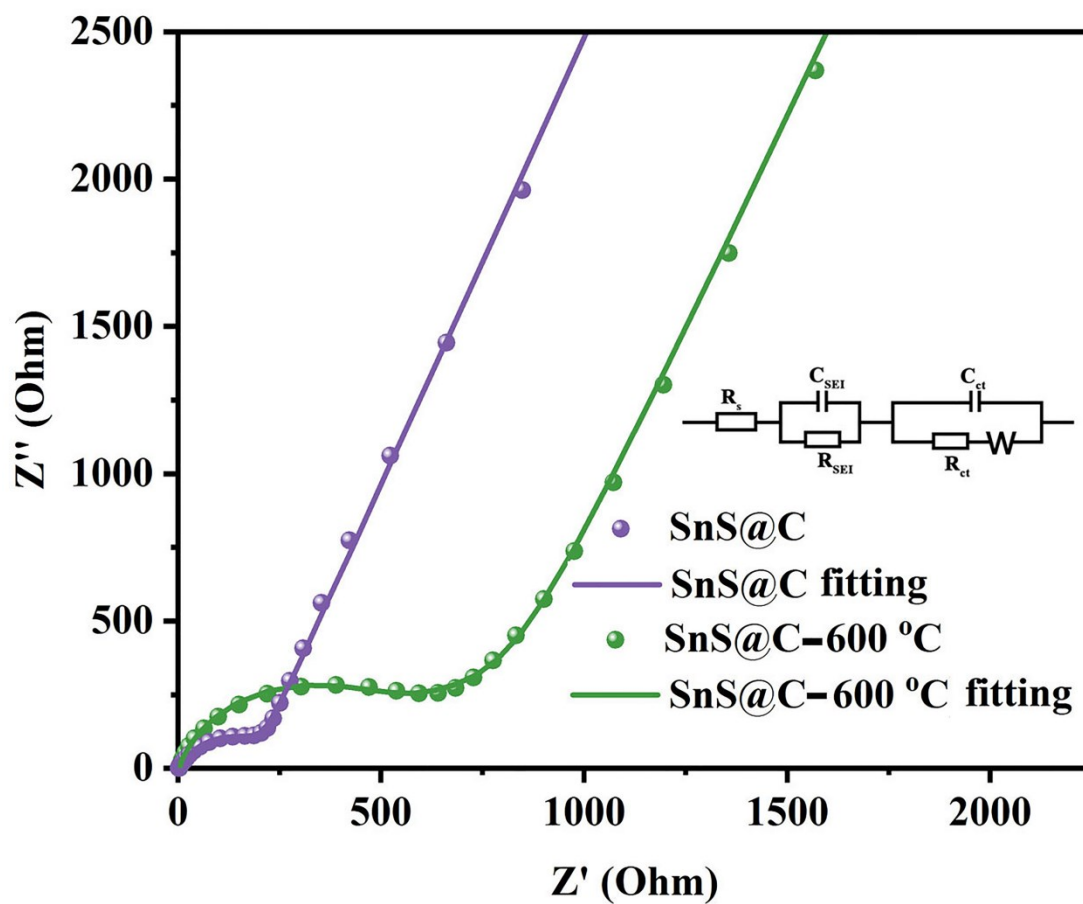


Fig. S14 Nyquist plots and equivalent circuit model for SnS@C and SnS@C-600 °C anodes for LIBs.

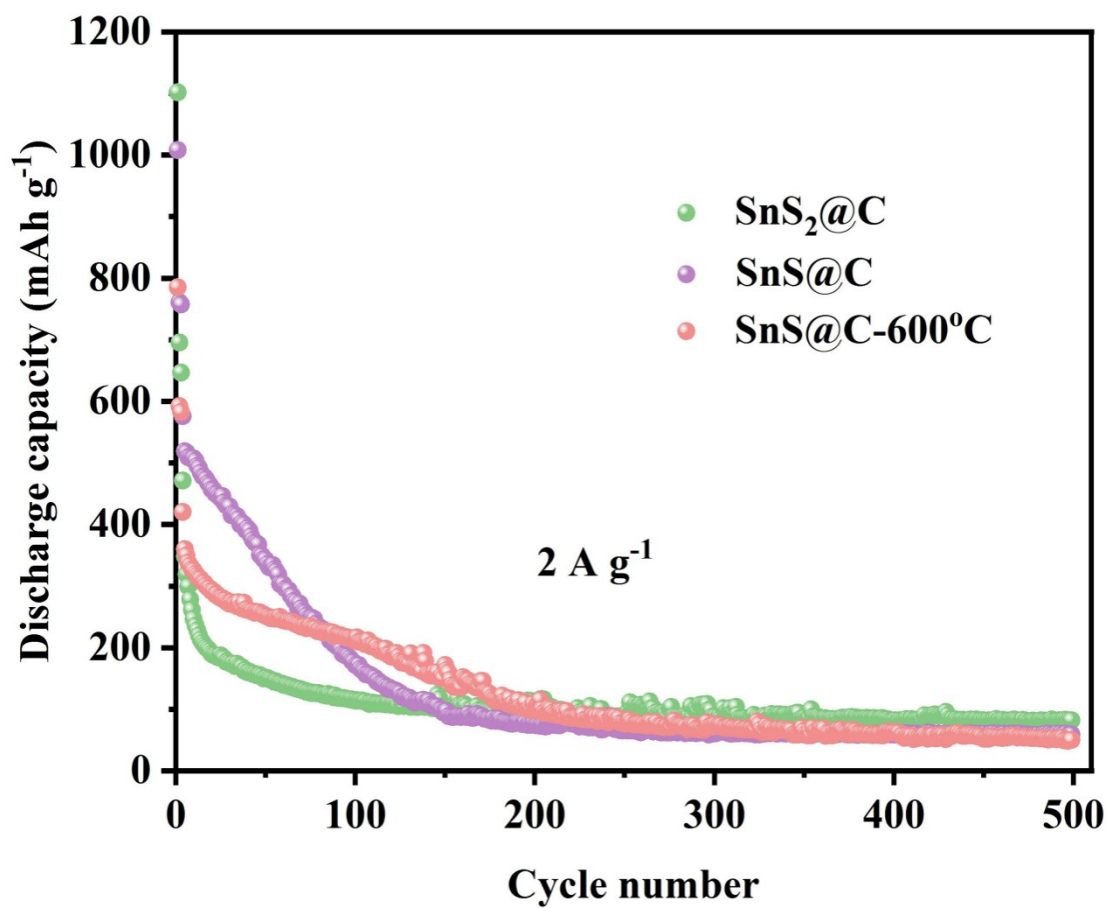


Fig. S15 Cycling performances of SnS₂@C, SnS@C and SnS@C-600 °C at a current density of 2 A g⁻¹.

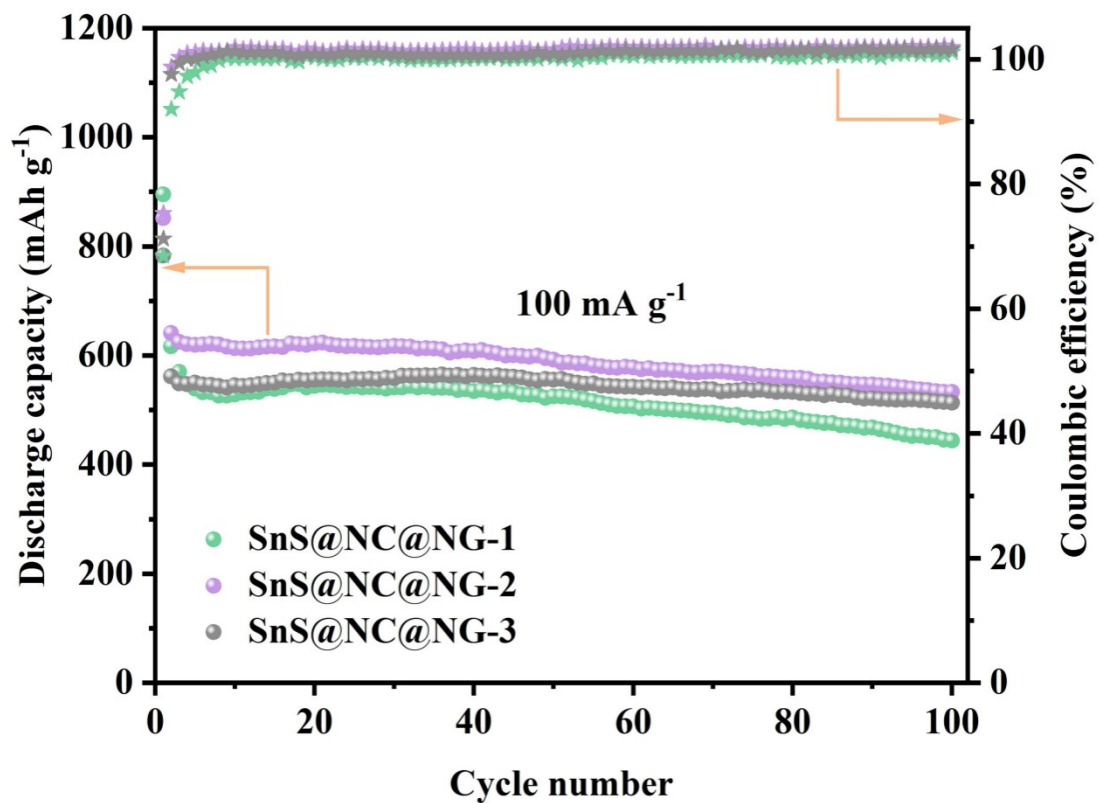


Fig. S16 Cycling performances of SnS@NC@NG with various NG content (SnS@NC@NG-1, SnS@NC@NG-2 and SnS@NC@NG-3) at a current density of 100 mA g⁻¹ for NIBs.

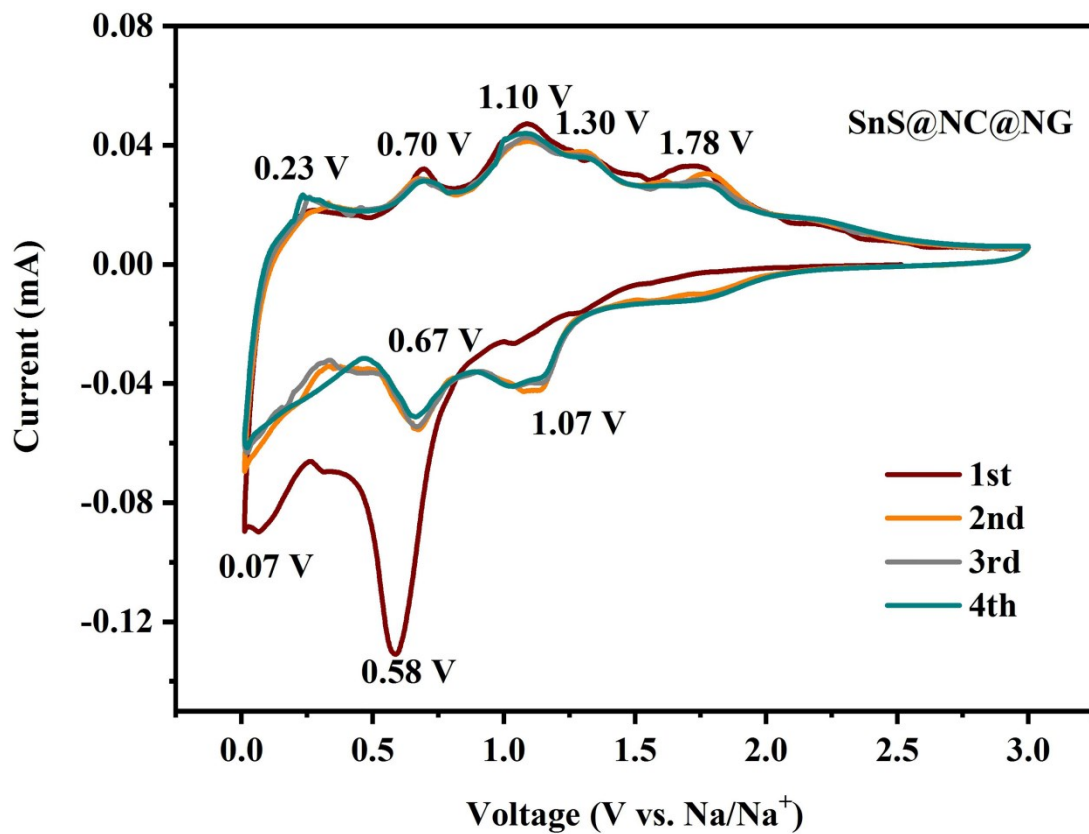


Fig. S17 Cyclic voltammograms profiles of SnS@NC@NG for NIBs at a scan rate of 0.1 mV s⁻¹.

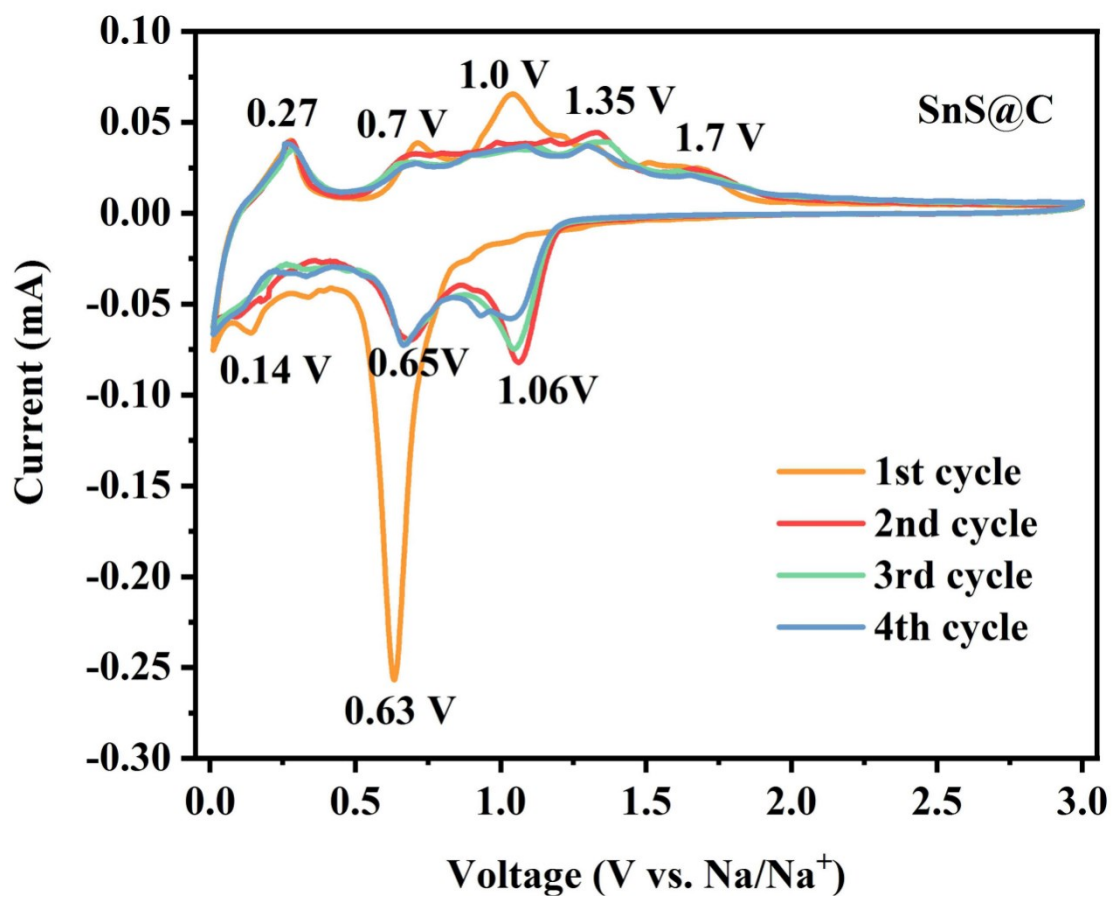


Fig. S18 Cyclic voltammograms profiles of SnS@C for NIBs at a scan rate of 0.1 mV s⁻¹.

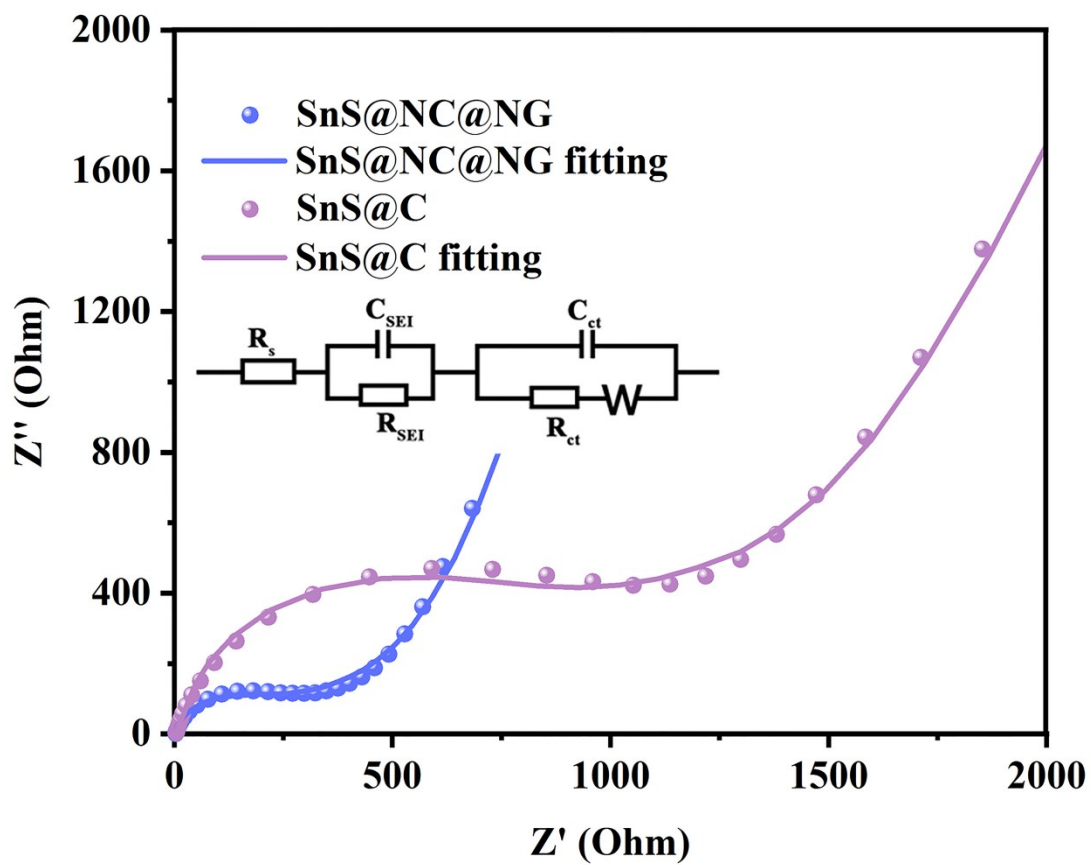


Fig. S19 Nyquist plots and equivalent circuit model for SnS@C and SnS@C-600 °C anodes for LIBs.

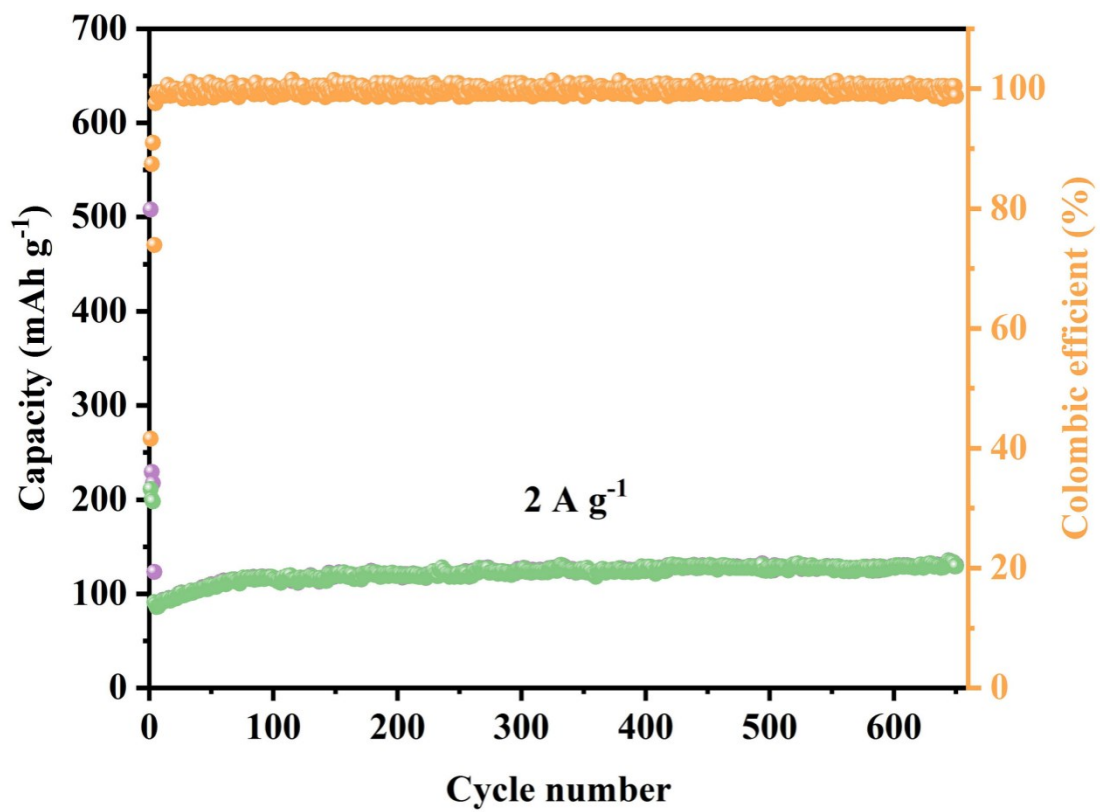


Fig. S20 Cycling performance of NC@NG for NIBs at 2 A g⁻¹.

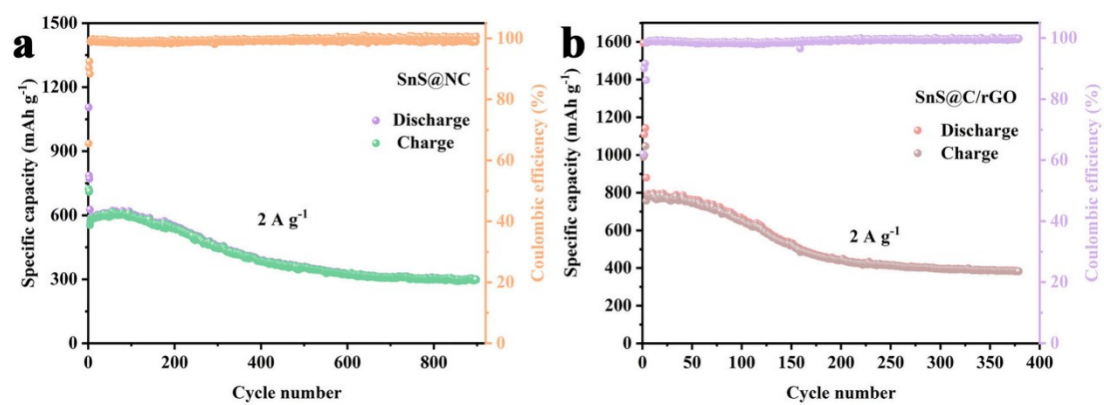


Fig. S21 Cycling performances of (a) SnS@NC and (b) SnS@C/rGO at current density of 2 A g⁻¹ for NIBs.

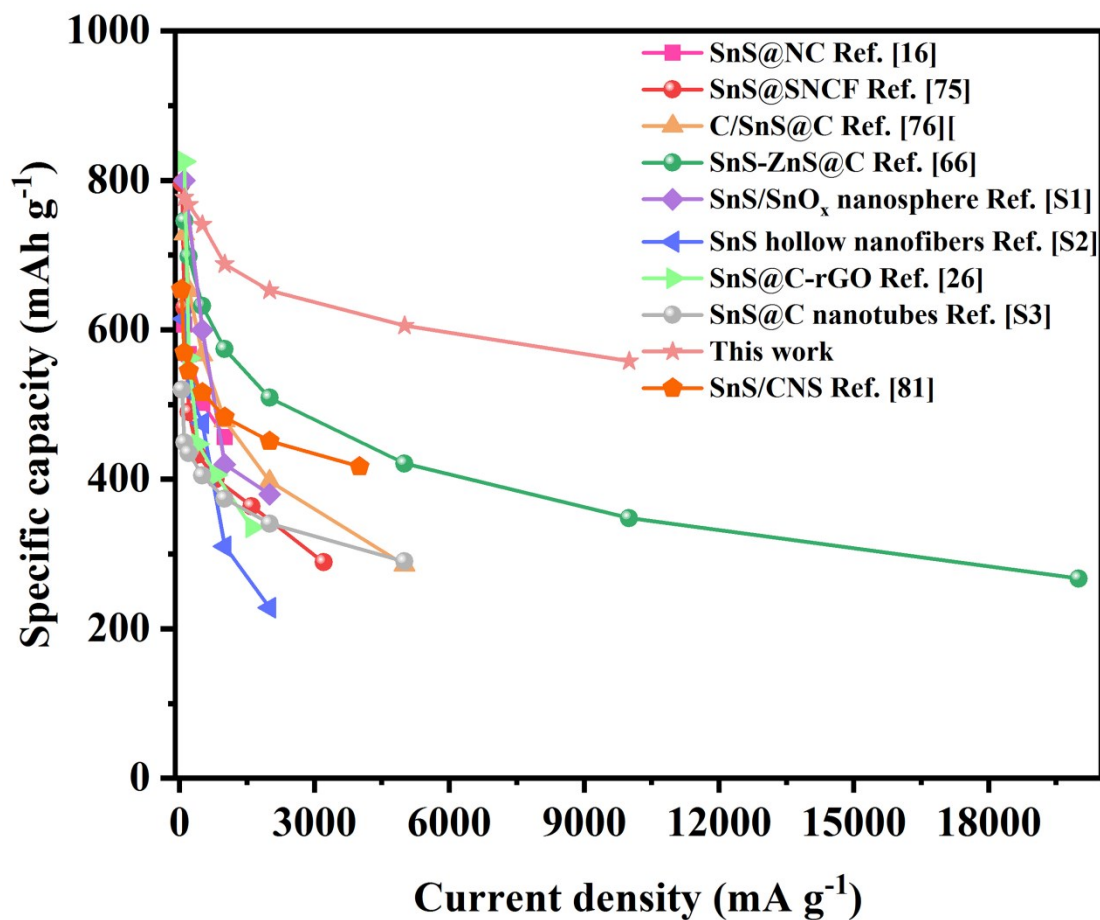


Fig. S22 Comparison of rate performance for NIBs between SnS@NC@NG electrode and the recently reported values for typical SnS-based anode materials.

Supplementary references

- S1 H. Bian, Z. Li, X. Xiao, P. Schmuki, J. Lu and Y. Y. Li, *Adv. Funct. Mater.*, 2019, **259**, 1901000.
- S2 H. Jia, M. Dirican, N. Sun, C. Chen, P. Zhu, C. Yan, X. Dong, Z. Du, J. Guo, Y. Karaduman, J. Wang, F. Tang, J. Tao and X. Zhang, *Chem. Commun.*, 2019, **55**, 505-508.
- S3 P. He, Y. J. Fang, X.-U. Yu and X. W. Lou, *Angew. Chem. Int. Ed.*, 2017, **56**, 12202-12205.